Hindawi
Advances in Civil Engineering
Volume 2019, Article ID 4978359, 14 pages
https://doi.org/10.1155/2019/4978359

Research Article

Investigation of the Insulation Effect of Thermal Insulation Layer in the Seasonally Frozen Region Tunnel: A Case Study in the Zuomutai Tunnel, China

Pengyu Zhao, Jianxun Chen, Yanbin Luo, Lijun Chen, Yao Li, and Chuanwu Wang

School of Highway, Chang'an University, Xi'an, Shaanxi 710064, China

Correspondence should be addressed to Jianxun Chen; chenjx1969@chd.edu.cn and Yanbin Luo; lyb@chd.edu.cn

Received 25 May 2019; Revised 5 August 2019; Accepted 23 August 2019; Published 30 September 2019

Academic Editor: Raffaele Landolfo

In this study, a field temperature test was performed to reveal the insulation effect of the thermal insulation layer installed at lining surface. The thermal insulation layer is made of polyphenolic, and the thickness is 7 cm. According to the test results, the temperature of the thermal insulation layer and lining continuously changes with the air temperature in the tunnel in an approximately trigonometric function. The temperature of tunnel lining without thermal insulation layer is close to the air temperature, which results in the lining frost in winter. The maximum temperature difference between the two sides of the thermal insulation layer can be 27°C. In the section whose buried depth is more than 11.4 m, the temperature of lining with thermal insulation layer in winter is mainly influenced by the cold air in the tunnel. When the monthly mean and lowest daily mean air temperature are lower than −10°C and −14.3°C in the coldest month, the temperature at the inner side of the thermal insulation layer is below 0°C. When the buried depth is less than 11.4 m, the temperature of lining is also influenced by the low temperature at ground surface. The temperature of lining is lower. The thicker thermal insulation layer and even active heat measure are needed. Therefore, the design of thermal insulation layer thickness should consider the air temperature distribution and tunnel buried depth along the tunnel length.

1. Introduction

To date, numerous cold region tunnels have been built in North Europe, North America, Japan, and China. Under the influence of periodic negative and positive temperatures, damage and cracking of concrete structure will occur [1–3]. Moreover, if the tunnel is underground, groundwater usually exists. In cold season, the groundwater in the lining structure or rock mass will freeze and the frost heave is formed [4], which continuously aggravates tunnel lining damage and cracking. Then, concrete peeling off (Figure 1(a)) and leakages will occur, and icicles and pavement icing are formed at low temperature (Figures 1(b) and 1(c)) [5–8]. Such damages increase the investment for tunnel maintenance, threaten traffic safety, and shorten tunnel service life [9].

Low temperature and groundwater are the two necessary conditions for the occurrence of tunnel frost damage. The groundwater situation in tunnels is complicated. Therefore, the main measure to prevent tunnel frost damage is to control tunnel temperature at present, such as thermal insulation doors [10], electric heat tracing [11], ground heat exchanger [12, 13], and thermal insulation layer. The thermal insulation layer with a light-weight insulation material is easily constructed with less investment and does not affect tunnel traffic. Therefore, it is extensively applied in the cold region tunnel to prevent the tunnel lining and rock mass frost [14–19].

At present, there are two different ways to install the thermal insulation layer in the tunnel. One method is installing the thermal insulating layer between the primary and secondary linings; the other method is installing the thermal

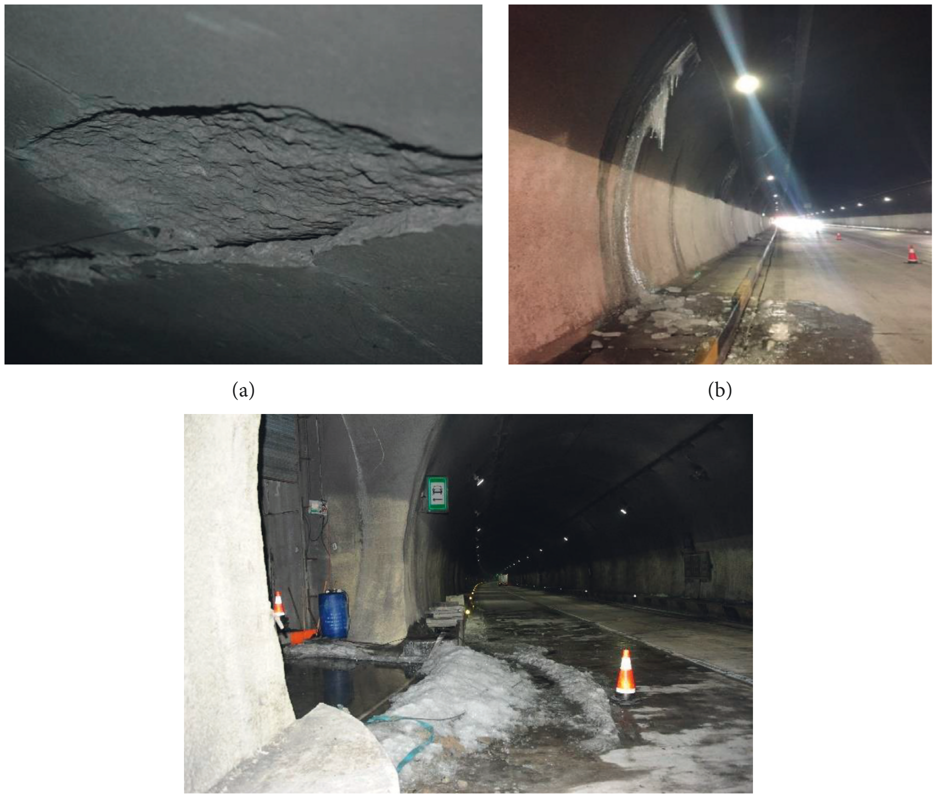

(a) (b)

(c)

Figure 1: Tunnel frost damage in cold region. (a) Tunnel lining concrete peeling off. (b) Tunnel leakage and icicles. (c) Tunnel pavement icing.

insulating layer at the surface of the secondary lining. Ma et al. proved that the two ways can provide an effective insulation effect to prevent tunnel frost damage based on the numerical calculation results [20]. However, considering the reliability, it is better to lay the thermal insulation layer at the secondary lining surface. The ambient air temperature outside the Zhegushan tunnel in China could be −20°C. A 4 cm-thick thermal insulation layer made of polyurethane whose thermal conductivity is 0.027 W/(m·k) was installed at the tunnel lining surface. Based on the results of finite element numerical calculation and field temperature measurement, it was verified by Xie et al. that the thermal insulation layer is enough to keep the temperature of tunnel lining higher than 0°C in winter [21]. Tan et al. established a numerical calculation model considering the ice-water phase change to calculate the temperature of the Galongla tunnel in China [22]. The lowest ambient air temperature outside the tunnel could be −28°C. The calculation results show that the 6 cm-thick polyphenolic insulation layer whose thermal conductivity is 0.025 W/(m·k) can prevent the tunnel lining and surrounding rock from freezing-thawing damage. Song et al. established a two-dimensional finite element calculation model to analyze the insulation effect of the thermal insulation layer with different thicknesses installed at tunnel lining surface [23]. The thermal conductivity of the thermal insulation layer is 0.025 W/(m·k). The results show that the thermal insulation layers with thicknesses of 5 cm and 7 cm can increase 4.85°C and 5.8°C temperature, respectively, to prevent the Houanshan tunnel frost. Li et al. established a coupled heat-water model to calculate the optimal thickness of the thermal insulation layer with a thermal conductivity of 0.025 W/(m·k) for the Jiangluling tunnel in China [24]. The lowest ambient air temperature outside the tunnel is lower than −15°C. The calculation results show that the 8.5 cm-thick thermal insulation layer can ensure the tunnel without frost risk. Yan et al. calculated the optimal thickness of the thermal insulation layer with a thermal conductivity of 0.024 W/(m·k) for the Dege tunnel in China through numerical calculation [25]. The lowest ambient air temperature outside the tunnel is approximately −20°C. The calculation results show that the 4 cm-thick thermal insulation layer is enough to prevent the tunnel lining frost. Yu et al. took the Huitougou tunnel in China as an example and analyzed the influences of thermal conductivity and thickness of the thermal insulation layer on tunnel temperature through numerical calculation [26]. The air temperature load in the tunnel in winter was selected as −20°C. The results show that the temperature of tunnel lining is close to 0°C in winter, when the thermal insulation layer whose thickness and thermal conductivity are 5 cm and 0.02 W/(m·k), respectively, is installed at the lining surface. In view of the above analysis, the insulation effect of the thermal insulation layer has been verified through a lot of numerical calculations. However, the majority of the research results lack the evidence from field temperature measurement. Moreover, the insulation limit or the applicable air temperature condition of the thermal insulation layer was not proposed in these studies.

According to the field temperature measurement results in the Tianhengshan tunnel in China, Luo found that the temperature at the waterproof board between the secondary and primary linings was still below 0°C in winter, although a 5 cm-thick thermal insulation layer made of polyurethane was installed at the lining surface [27]. The groundwater in the tunnel would freeze in winter, and the frost heave load would act on the tunnel lining. Feng et al. investigated the reliability of the 5 cm-thick thermal insulation layer that was installed at the lining surface of the Yuximolegai tunnel in China, through field temperature measurement and physical model test [28, 29]. Based on the temperature distribution in the tunnel lining and rock mass, it can be found that the 5 cm-thick thermal insulation layer whose thermal conductivity is 0.03 W/(m·k) can only stop about 86.5% of the lowest temperature, and there is still a freezing depth of approximate 0.5 m in the rock mass. The ideal thickness of the thermal insulation layer was calculated to be 27 cm through numerical calculation, which is difficult to achieve in the actual tunnel engineering. On the basis of the temperature distributions in the lining and rock mass in the Wusongling tunnel and Tianhengshan tunnel, Lai et al. proposed that the insulation effect of the thermal insulation layer is limited. Only the thermal insulation layer hardly eliminates tunnel frost damage, and the relevant active heating measures, such as electric heat tracing and ground heat exchanger, should be combined [11, 30]. Therefore, the actual insulation effect of the thermal insulation layer is not clear at present, and no consensus has been established.

In this paper, a comprehensive temperature measurement was conducted along the length of the Zuomutai tunnel in the Hegang-Dalian highway (G11) in China. The temperature change rules of air, thermal insulation layer, and lining in the tunnel were investigated. The actual insulation effect of the thermal insulation layer was analyzed on the basis of the temperature changes of the thermal insulation layer and lining under different air temperature loads in different monitoring sections. The results can provide references for thermal insulation layer thickness design in seasonally frozen region tunnels.

2. Project Profile

2.1. Test Site and Climate. The Zuomutai tunnel in the Hegang-Dalian highway is located in the north of Changbai Mountain in Jilin, China, as depicted in Figure 2. It was completed in October 2016. Two northwest and south bound separated tunnels were designed. The south bound tunnel was chosen as the test object in this study. The length of the tunnel is 2910 m, which is from K628 + 536 (tunnel entrance at the Hegang side) to K631 + 446 (tunnel exit at the Dalian side). The traffic volume of the tunnel is small, and the mechanical ventilation machines are not always turned on. Therefore, the natural wind dominates in this tunnel affect the tunnel temperature. The elevation at the tunnel entrance is higher than that at the tunnel exit. The height difference is 28 m.

The tunnel location is in the seasonally frozen region, where the minimum annual average temperature is from 2005 to 2014 is 3.8°C, and the lowest monthly mean temperature is −16.1°C. In accordance with the classification of tunnel frost damage by Luo et al. [27, 31], the coldness of the tunnel belongs to "severe cold" level. The serious (V level) tunnel frost damage easily occurs. The thermal insulation layer is necessary to be installed to prevent tunnel frost damage.

2.2. Thermal Insulation Layer Installation. The thermal insulation layer in this tunnel is installed at the tunnel secondary lining surface, as shown in Figure 3. The insulation board is made of polyphenolic material whose thermal conductivity is 0.026 W/(m·k). The thickness of the thermal insulation board is 7 cm. The thermal insulation boards are installed at the lining surface through expansion bolts, U-shaped steel components, and steel keels (Figure 4). Fireproof boards are set outside the thermal insulation boards, which are installed at the steel keels through tapping screws. Fire retardant coatings are sprayed at the outer surface of fireproof boards. The installation lengths of the thermal insulation layer are 450 m and 830 m at the tunnel entrance and exit, respectively.

3. Tunnel Temperature Test

3.1. Test Scheme. The resistance temperature sensors of PT100 A (A level platinum resistor sensor) (Figure 5) with a large measuring range, fast temperature response, and good stability were applied to measure the temperature of the tunnel. All the sensors were calibrated before installation to ensure the measurement accuracy. The temperature test equipment was developed through introducing integrated electric chips to achieve automatic temperature test. On the basis of the accuracy analysis, the final temperature test error is less than 0.29 and may even be less than 0.06°C [32]. The test frequency was set as 20 minutes.

The sensors were installed during thermal insulation layer construction. The temperature monitoring system was arranged along the full length of the tunnel. Given the significant temperature variation at the area approaching the tunnel portal, the interval between monitoring sections is small. With the increase of the distance from the tunnel portal, the interval between monitoring sections increases. Three measuring points are set at the vault (height from the pavement of 7.1 m), waist (height from the pavement of 5.4 m), and side wall (height from the pavement of 1.6 m) in every monitoring section. The specific layout of the monitoring sections and sensors is presented in Figure 6. The air temperature in the tunnel and the temperature at different surfaces of the thermal insulation layer and inside the tunnel lining (15 cm from the lining surface) were measured.

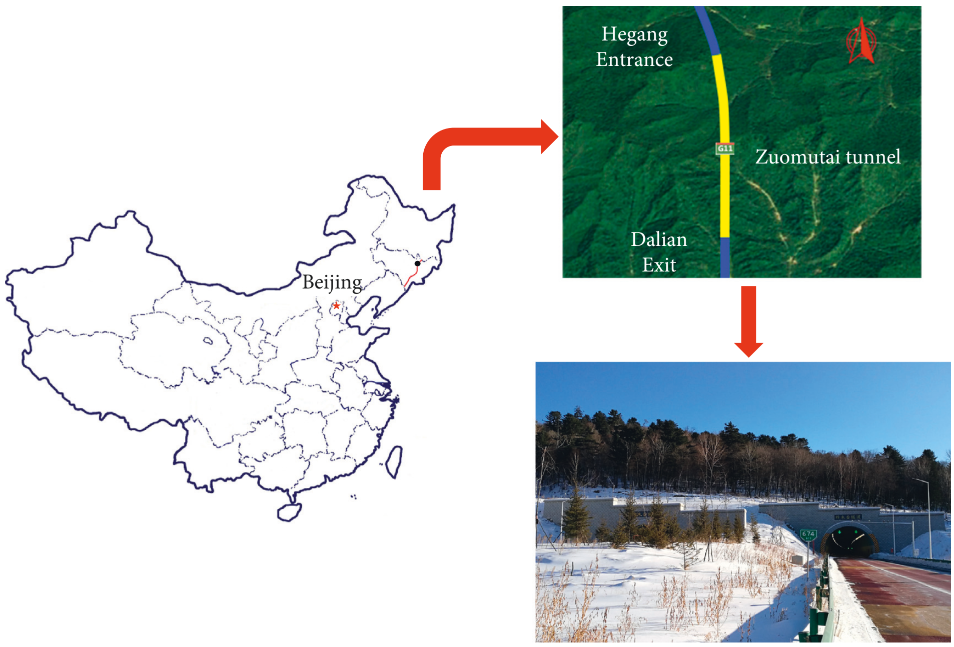

FIGURE 2: Zuomutai tunnel.

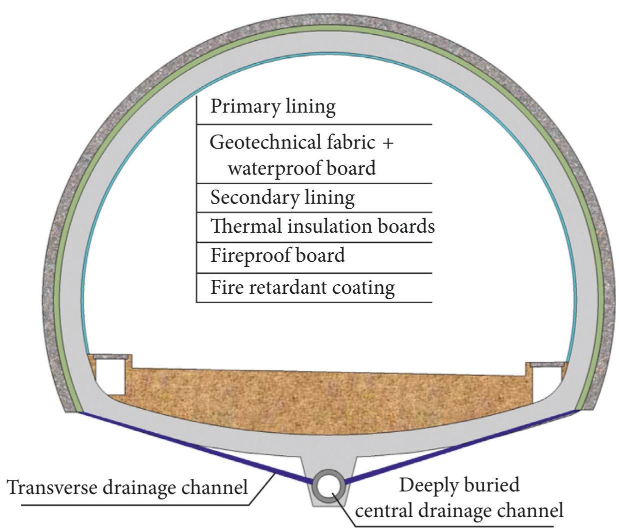

FIGURE 3: Tunnel lining, thermal insulation layer, and drainage.

In addition, an automatic meteorological observation station was set at both outsides of the tunnel entrance and exit, which is approximately 50 m away from the tunnel portal. The meteorological observation station can automatically monitor the ambient air temperature, wind direction, and velocity outside the tunnel. The test frequency is 1 minute.

3.2. Test Results

3.2.1. Temperature Change over Time. Figure 7 shows that the daily mean air temperature changes at both outsides of the tunnel entrance and exit with the date increasing from January 2017 to April 2018 (more than a whole year time). The overall temperature change rules at both outsides of the tunnel are coincident and in an approximately trigonometric function. The temperature values are also close.

The typical sections of K628 + 541, K628 + 900, K629 + 091, K630 + 490, K630 + 690, and K631 + 441 in the tunnel were taken as examples. Due to the temperature changes at the different heights in the same monitoring section are similar, only the daily mean temperature changes of the air, thermal insulation layer, and lining at the side wall of the typical sections with the date increasing from January 2017 to January 2018 are demonstrated in Figure 8.

Under the effect of the airflow outside the tunnel, the air temperature in different monitoring sections along the length of the tunnel changes with the ambient air temperature outside the tunnel, whose overall change rules are similar and in an approximately trigonometric function. The air temperature in January is lowest in the whole year. The temperature values of the air, fireproof layer surface, and outer surface of the thermal insulation layer are close in the sections with the thermal insulation layer, and the temperature change rules are coincident. However, the temperature differences between the inner and outer sides of the thermal insulation layer are large due to the great insulation effect of the thermal insulation layer. But, the heat transfer also occurs in the thermal insulation layer, which makes the temperature at the inner side of the thermal insulation layer continuously change with the air temperature. When the air temperature is lowest, the temperature at the lining surface and inside lining also reaches the lowest. However, the change amplitude of the temperature of lining is much smaller than that of the air.

In the sections where no thermal insulation layer is installed, the change rules of the temperature of the air and lining were completely coincident. Moreover, the temperature values of the air and lining are close. Therefore, the temperature of lining is low in winter.

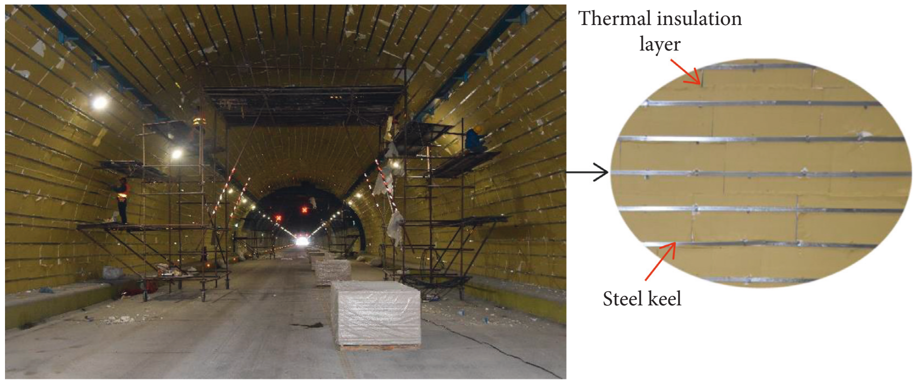

Figure 4: Installation of thermal insulation boards.

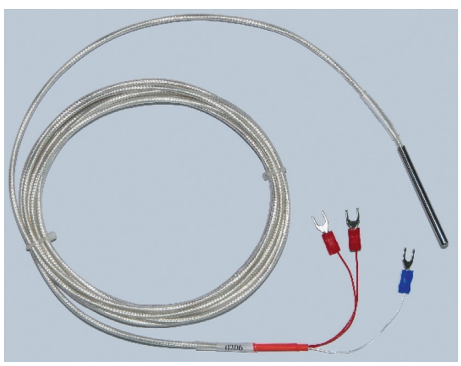

Figure 5: PT100 A sensors.

3.2.2. Temperature Distribution along the Tunnel Length. In winter, the cold air outside the tunnel will flow into the tunnel and influence the air temperature distribution in the tunnel. As such, the air temperature is negative within a certain length range inside the tunnel. Given that the air temperatures in January are lowest, only a statistics analysis of the wind directions and velocities at both outsides of the tunnel in January 2018 is conducted (Figure 9), and the distributions of monthly mean temperature of the air and lining along the tunnel length are illustrated in Figure 10.

The natural wind dominates in this tunnel, which is attributed to the excess static pressure difference, ventilation-wall pressure difference, and thermal potential difference [33, 34]. As the change rules of ambient air temperature at the both outsides of the tunnel are coincident and the temperature values are close, the excess static pressure difference in this tunnel mainly results from the atmospheric horizontal pressure gradient. However, the tunnel length is less than 3000 m. The excess static pressure difference in this tunnel is relatively low. When the natural wind blows to the tunnel, part of the wind pressure transforms into the airflow pressure in the tunnel, which causes the ventilation-wall pressure difference in the tunnel. On the basis of the wind test results, the winds outside the tunnel usually blew to the two sides of the tunnel in January 2018, that is, southerly and northerly winds prevailed outside the tunnel entrance and exit, respectively (Figure 9). Therefore, the ventilation-wall pressure at the tunnel entrance is intermittent or transient. The thermal potential difference is caused by temperature difference between inside and outside the tunnel. In winter, the air temperature inside the tunnel is higher than that outside the tunnel, which causes the air inside the tunnel to float up to the high elevation side and the cold air outside the tunnel to flow into the tunnel from the low elevation portal and out to the high elevation portal. Therefore, under the effect of thermal potential difference, the cold air outside this tunnel is always flowing into the tunnel from the exit and out to the entrance in winter. The air temperature at the tunnel exit is more influenced by the cold air outside the tunnel. As a result of the above, the monthly mean air temperature distributions inside the tunnel present an asymmetric inverted U-shaped pattern in the longitudinal direction of the tunnel in January 2018, as shown in Figure 10.

The lowest air temperature is at the tunnel exit, which is approximately −16°C. The air temperature at the tunnel entrance is much higher than that at the exit. The temperature difference between the tunnel entrance and exit is approximately −6°C at the side wall, and higher than −11°C at the vault and waist. The highest air temperature was approximately −5°C at the vault of the monitoring section K629 + 091, which is 555 m from the tunnel entrance. Both the air temperatures at the side wall and waist are approximately −6°C in this section. According to the previously proposed air temperature threshold values of 0°C [23, 25, 35, 36] or −5°C [35, 37] used to determine the length of thermal insulation layer length, the thermal insulation layer needs to be installed in the full length of the tunnel. It is inconsistent with the conventional design of tunnel thermal insulation layer length in China [38, 39], which is always approximately 1000 m.

Indeed, the temperature of lining drops abruptly in the sections without thermal insulation layer installed. In the section K629 + 091 where the air temperature is highest, the temperature inside lining is still lower than −2°C. In the section K630 + 490, the temperature inside lining is lowest, which is lower than −6°C. Moreover, field investigation shows that due to tunnel frost, tunnel lining cracking, leakage, and icicle have occurred in April 2017 in some sections without thermal insulation layer (Figure 11).

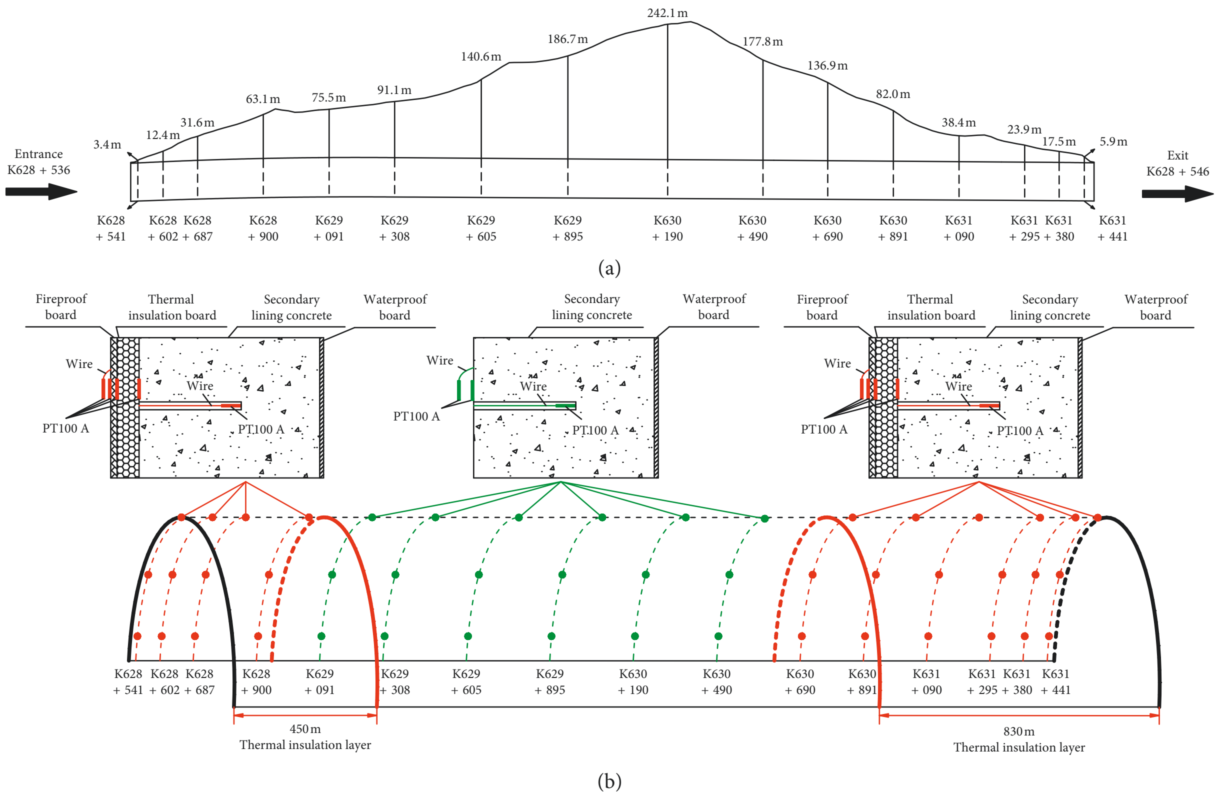

Figure 6: Layout of monitoring sections and sensors in the test tunnel. (a) Monitoring sections and their buried depths (from the tunnel vault lining surface to ground surface). (b) Sensors in the monitoring sections.

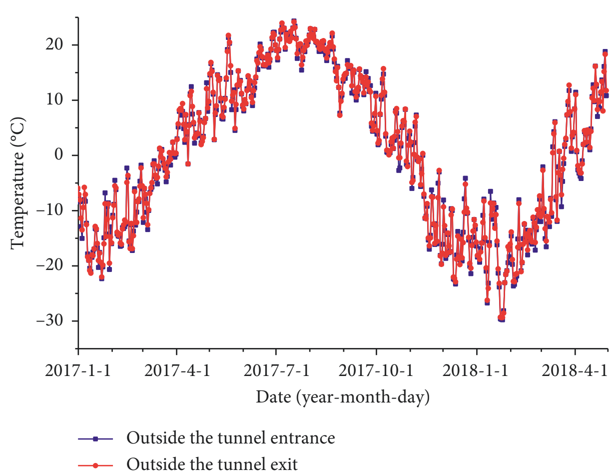

Figure 7: Daily mean air temperature changes at both outsides of the tunnel entrance and exit with the date increasing from January 2017 to April 2018.

With the distance from the tunnel exit increasing, the temperature of lining in the sections with thermal insulation layer increases with the air temperature increasing. However, due to the lower air temperature at the side of the tunnel exit, the temperature of lining in the sections is below 0°C, except the section K630 + 690. In addition, although the air temperature of the section K631 + 295 is close to that of the adjacent section K631 + 380, even a little higher, the temperature of lining in this section is much lower. Similarly, the air temperature of the adjacent sections K631 + 380 and K631 + 441 are also close. But, the temperature of lining at the vault in the section K631 + 441 is much lower. As the air temperature at the side of the tunnel entrance is higher, the temperature of lining in the sections with thermal insulation layer is higher than 2°C, except the section K628 + 541. In the section K628 + 541, the temperature of lining is much lower, especially at the vault where the temperature of lining is approximately −2.5°C. On the basis of the above analysis, the 7 cm-thick thermal insulation layer is not enough to prevent tunnel lining frost in most sections at the tunnel exit. While in the most of the sections at the tunnel entrance, the thickness of the thermal insulation layer is enough, even superfluous, to make the lining temperature higher than 2°C due to the higher air temperature.

4. Analysis of Insulation Effect of Thermal Insulation Layer

According to the above results of the temperature of lining along the tunnel length, the temperature of lining in the sections K628 + 541, K631 + 295, and K631 + 441 is much lower than that of the adjacent sections. Therefore, the temperature changes of lining with time in these three sections and the adjacent sections, in which the air temperature is close, were compared and analyzed. Figure 12 shows the changes of temperature inside lining at the tunnel

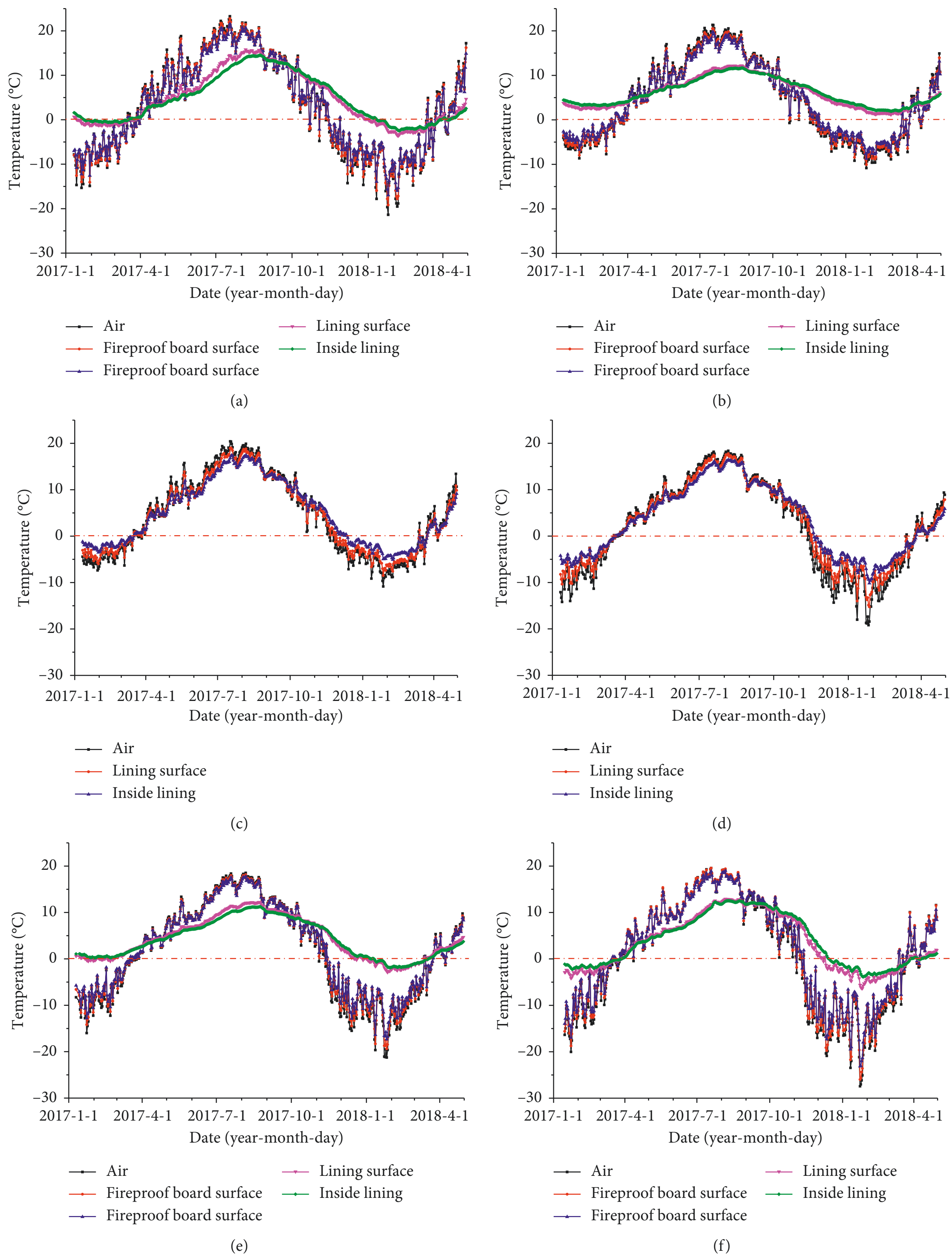

Figure 8: Daily mean temperature changes of the air, thermal insulation layer, and lining at the side wall in the typical monitoring sections with the date increasing from January 2017 to April 2018. (a) Section K628 + 541. (b) Section K628 + 900. (c) Section K629 + 091. (d) Section K631 + 490. (e) Section K630 + 690. (f) Section K631 + 441.

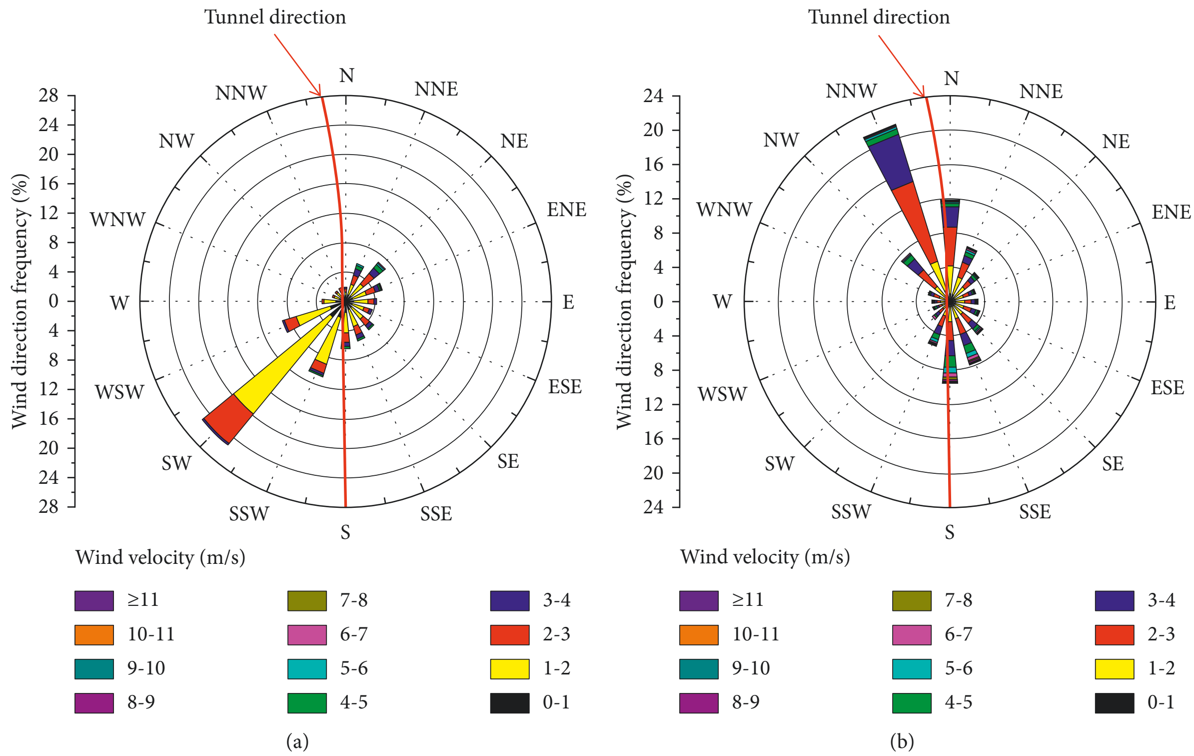

Figure 9: Rose diagrams of the frequency of wind direction and the wind velocity at both outsides of the (a) tunnel entrance and (b) exit in January 2018.

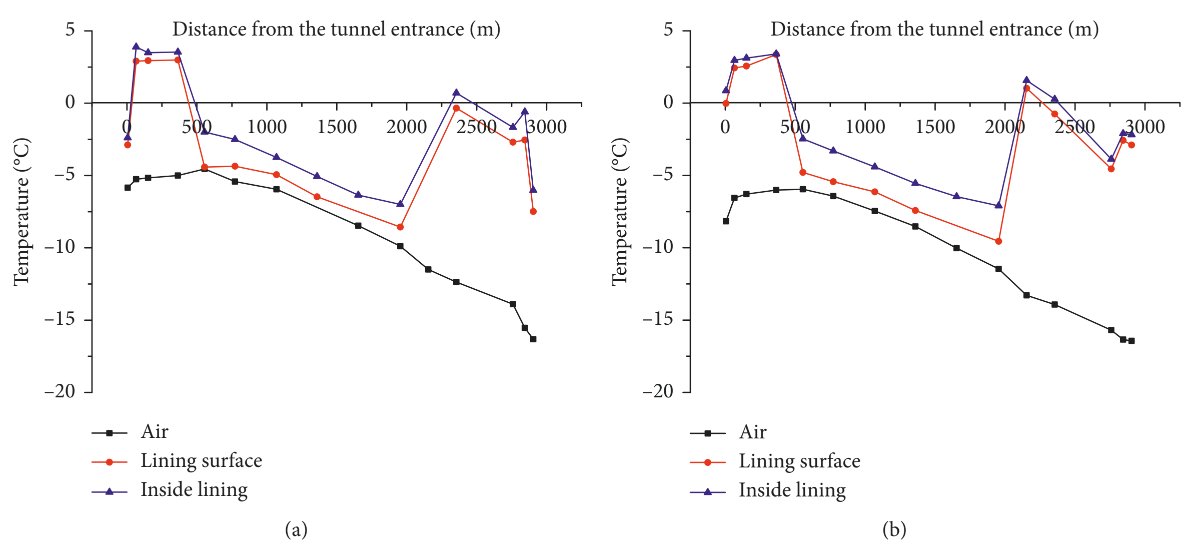

Figure 10: Continued.

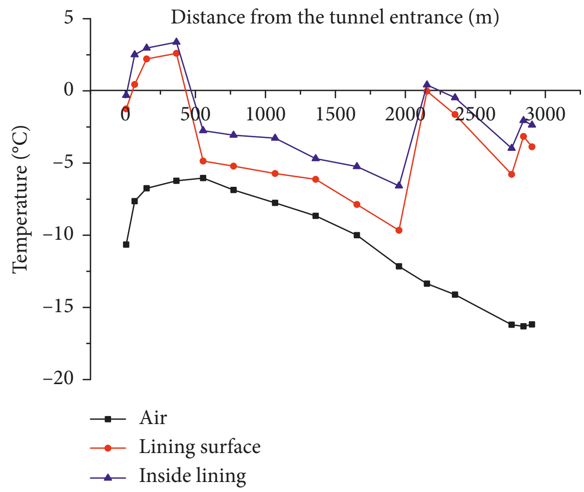

(c)

Figure 10: Distribution of the monthly mean temperature of the air and lining along the tunnel length in January 2018. (a) Vault. (b) Waist. (c) Side wall.

(a)

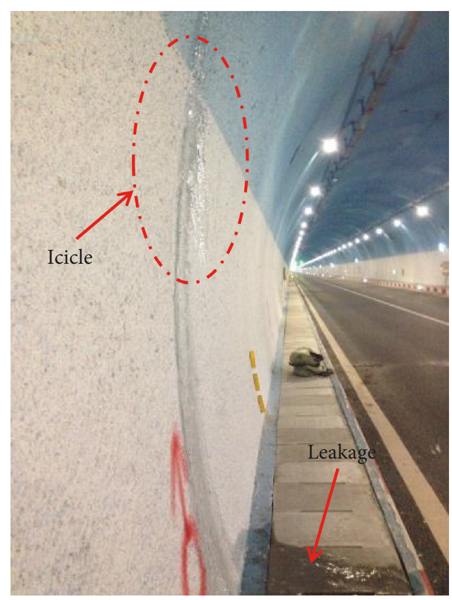

(b)

Figure 11: Tunnel frost damage in the sections without thermal insulation layer. (a) Near section K629 + 091. (b) Near section K630 + 490.

vault, waist, and side wall in the sections K628 + 541, K628 + 602, and K628 + 687 from January 2017 to April 2018. Figure 13 shows the changes of temperature inside lining in the sections K631 + 090, K631 + 380, and K631 + 441 from January 2017 to April 2018.

The temperature changes of lining in the sections K628 + 602 and K628 + 687 are coincident, and the temperature values are close. However, the temperature change amplitude of tunnel lining in the section K628 + 541 is much larger; that is, the temperature of lining in this section is much lower in winter and higher in summer. According to the tunnel design data, the buried depth of the section is only 3.4 m (Figure 6), which is much shallower than those of the sections K628 + 602 and K628 + 687 of 12.1 m and 30.9 m, respectively. Therefore, the temperature of lining in the section K628 + 541 is influenced by the temperature of the ground surface, which causes the larger temperature change amplitude, especially at the vault. The buried depths are larger at the waist and side wall, which are 5.1 m and 8.9 m, respectively. The influence of the temperature at the ground surface is less. Correspondingly, the change amplitudes of temperature inside the tunnel lining are smaller. Similarly, the buried depth of the section K631 + 441 is only 5.9 m. It is much shallower than the two adjacent sections K631 + 090 and K631 + 380, where the buried depths are more than 17.5 m. Therefore, under the effect of the temperature at the

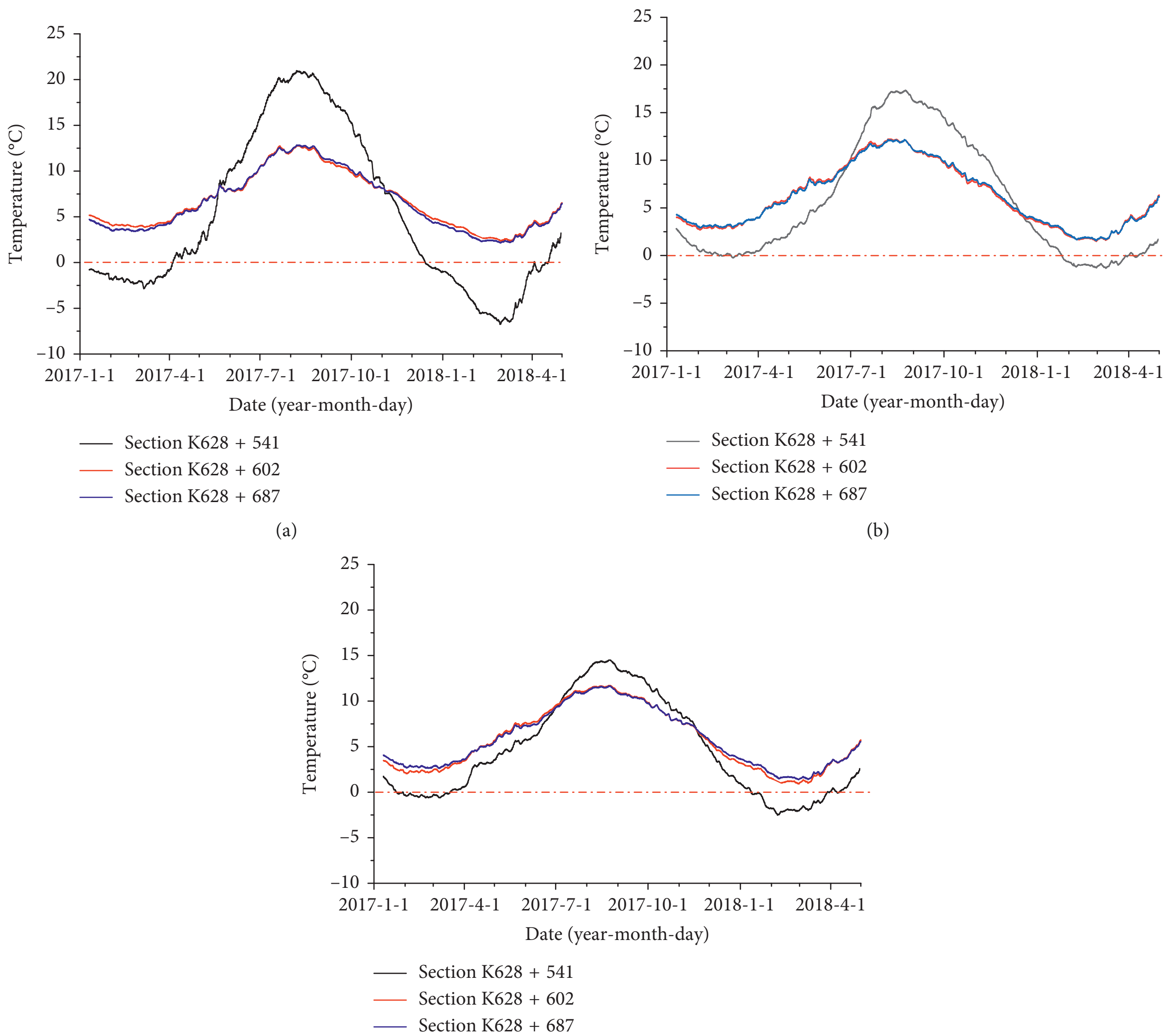

(a) (b) (c)

Figure 12: Changes of temperature inside lining at the tunnel vault, waist, and side wall in the sections K628 + 541, K628 + 602, and K628 + 687 from January 2017 to April 2018. (a) At vault. (b) At waist. (c) At side wall.

ground surface, the temperature change amplitude of the tunnel lining in the section K631 + 441 is also larger. The temperature change amplitudes at the waist and side wall are smaller than that at the vault in this section because of the larger buried depth. Moreover, the temperature change amplitude of lining at the side wall with the buried depth of 11.4 m is close to those of the two adjacent sections. Especially in winter, the temperature changes of lining at the side wall in the two sections K631 + 441 and K631 + 380 are coincident, and the temperature values are very close, due to the thermal insulation of snow at the ground surface. Therefore, when the buried depth is larger than 11.4 m, the influence of low temperature at the ground surface on the tunnel with thermal insulation layer installed is little in winter. The temperature of lining is mainly influenced by the cold air in the tunnel.

In addition, the temperature change amplitudes of tunnel lining in the section K631 + 295 are larger than that in the adjacent section K631 + 380 in the whole year. It may be caused by the poor construction quality and low insulation effect of the thermal insulation layer.

On the basis of the above, a statistics analysis of the temperature of the air and lining in the monitoring sections with thermal insulation layer was conducted, excluding the test results in the sections K628 + 541, K631 + 295, and K631 + 441. Table 1 shows the statistic results of the monthly and lowest daily mean air temperature and the lowest temperature of the air and lining surface in the monitoring sections in January 2017 and 2018.

According to the results of Table 1, the temperature difference between the inner and outside sides of the thermal insulation layer, namely, the difference between the lowest

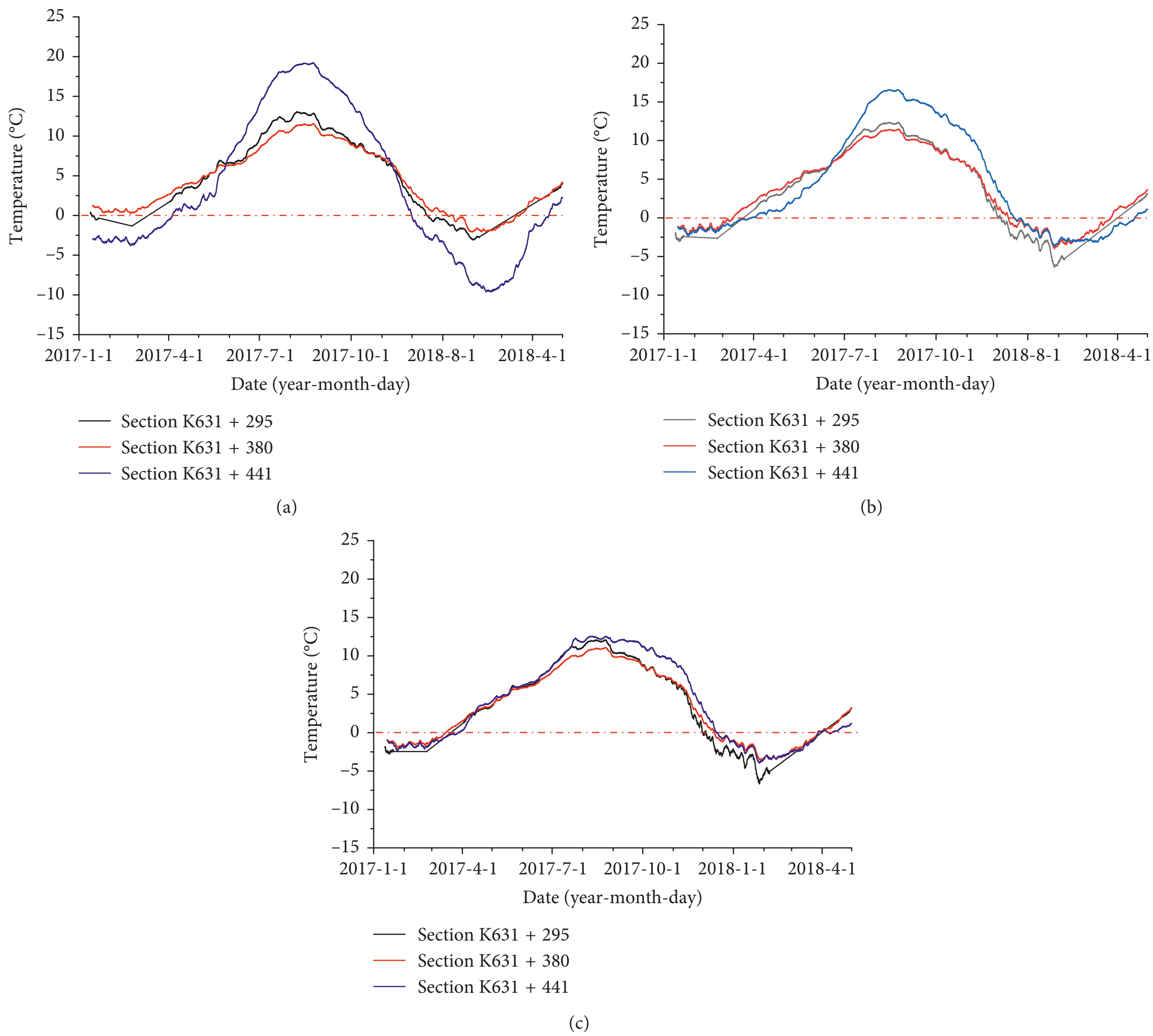

Figure 13: Changes of temperature inside lining at the tunnel vault, waist, and side wall in the sections K631 + 090, K631 + 380, and K631 + 441 from January 2017 to April 2018. (a) At vault. (b) At waist. (c) At side wall.

temperature of air and lining surface, is higher than 14°C. The maximum temperature difference can reach 27°C. The air temperature in the tunnel is constantly changing. However, the heat transfer in the thermal insulation layer is slow and takes time, due to the great insulation effect of the thermal insulation layer. Therefore, the transient air temperature load cannot cause significant temperature change at the back of the thermal insulation layer. The correlation between the lowest temperature of the air and lining surface is not good. It cannot accurately reveal the insulation effect of the thermal insulation layer. The temperature of lining changes continuously with the air temperature in the tunnel. Moreover, when the daily mean air temperature changes dramatically in winter, the daily mean temperature of lining fluctuates accordingly, as shown in Figure 8. Therefore, the data of monthly and lowest daily mean air temperature are selected and compared with the lowest temperature at the lining surface, in order to investigate the insulation effect of the thermal insulation layer. According to the data in Table 1, the correlations between the monthly mean air temperature, lowest daily mean air temperature, and lowest temperature at the lining surface are shown in Figures 14 and 15, respectively.

There is a strong linear polynomial relationship between the coldest monthly mean air temperature and the lowest temperature at the lining surface with thermal insulation layer. The square of the adjusted correlation coefficient R2 is 0.95. When the monthly mean air temperature is lower than −10°C, the temperature at the lining surface can be below 0°C. There is a linear relationship between the lowest daily mean air temperature in the coldest month and the lowest temperature at the lining surface. The square of the adjusted correlation coefficient R2 is 0.96. When the lowest daily mean air temperature is lower than −14.3°C, the temperature

Table 1: Monthly and lowest daily mean air temperature and lowest temperature of the air and lining surface in the sections with thermal insulation layer in January 2017 and 2018.

Sections		Monthly mean air temperature (°C) (2017/2018)	Lowest daily mean air temperature (°C) (2017/2018)	Lowest air temperature (°C) (2017/2018)	Lowest temperature at lining surface (°C) (2017/2018)
K628 + 602	Vault	−5.4/−5.4	−8.3/−9.3	−15.2/−19.6	2.8/1.8
	Waist	−6.7/−6.7	−10.1/−10.5	−20.2/−22.8	2.0/1.2
	Side wall	−7.6/−7.8	−11.7/−12.8	−21.1/−25.7	—/—
K628 + 687	Vault	−4.7/−5.3	−7.5/−9.2	−13.2/−16.4	2.8/2.0
	Waist	−6.4/−6.4	−9.4/−10.5	−17.0/−20.3	2.3/1.2
	Side wall	−6.8/−6.9	−10.4/10.7	−18.3/−19.7	1.6/0.9
K628 + 900	Vault	−4.9/−5.1	−6.8/−9.2	−11.3/−13.4	3.0/2.1
	Waist	−5.8/−6.2	−8.0/−10.5	−15.0/−17.7	3.2/2.3
	Side wall	−6.2/−6.4	−8.6/−10.8	−15.1/−17.9	2.2/1.4
K630 + 690	Vault	−9.9/−11.5	−12.9/−18.1	−20.3/−24.3	—/—
	Waist	−11.7/−13.3	−15.9/−21.1	−22.2/−26.8	0.5/−1.6
	Side wall	−11.6/−13.4	−16.0/−21.2	−22.2/−27.0	−0.7/−3.3
K630 + 891	Vault	−9.6/−12.4	−13.1/−18.1	−20.2/−24.6	0.59/−1.9
	Waist	−11.4/−13.9	−16.8/−22.5	−23.1/−27.9	−0.4/−2.6
	Side wall	−12.8/−14.1	−18.3/−22.8	−24.4/−28.3	−1.2/−3.7
K631 + 090	Vault	−10.6/—	−15.1/—	−22.1/—	−0.3/—
	Waist	−12.1/—	−18.1/—	−24.5/—	—/—
	Side wall	−12.3/—	−18.2/—	−24.4/—	−3.7/—
K631 + 380	Vault	−12.7/−15.5	−18.9/−24.8	−26.1/−30.8	−2.0/−5.1
	Waist	−13.5/−16.3	−20.3/−27.1	−26.5/−32.0	−3.2/−5.0
	Side wall	−13.6/−16.3	−20.0/−26.8	−27.0/−31.6	−5.0/−5.2

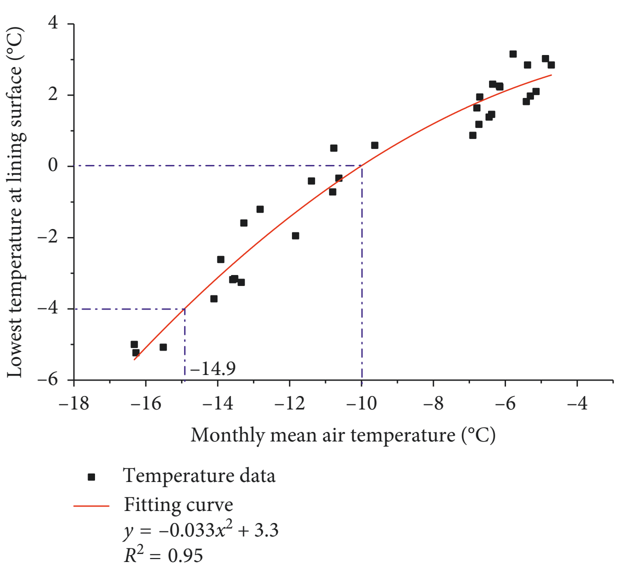

Figure 14: Correlation between the monthly mean air temperature and the lowest temperature at the lining surface in January (the coldest month).

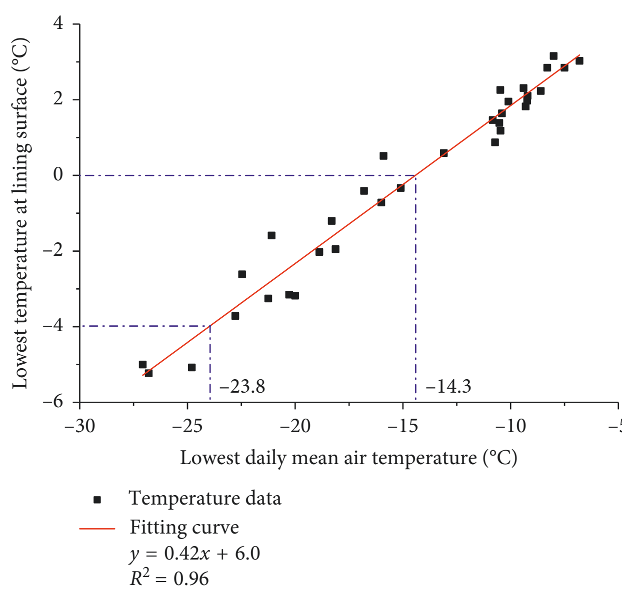

Figure 15: Correlation between lowest daily mean air temperature and the lowest temperature at the lining surface in January (the coldest month).

at the lining surface can be below 0°C. On basis of the above, the lining temperature changes in these sections in Table 1, whose buried depths are all higher than 12.5 m, are mainly attributed to the air temperature changes in the tunnel. When the monthly mean and lowest daily mean air temperature in January are lower than −10°C and −14.3°C, respectively, the temperature at the lining surface is below 0°C.

5. Conclusions

In this study, the field temperature measurement, including the temperature in the air, thermal insulation layer, and lining, was performed along the length of the tunnel. The temperature change rules and distribution characteristics in the tunnel were analyzed. The insulation effect of the thermal insulation layer was investigated. Some conclusions are drawn as follows:

(1) The temperature of air and lining is close in the section without thermal insulation layer. As the monthly mean air temperature in the whole tunnel is below −5°C in January, the temperature inside tunnel lining (from the lining surface 15 cm) is lower than −2°C. Therefore, the thermal insulation layer needs to be installed in the whole tunnel to prevent tunnel lining frost, even the tunnel length is approximately 3 km.

(2) The temperature of the thermal insulation layer changes with the air temperature in an approximately trigonometric function. The maximum temperature difference between the inner and outer sides of the thermal insulation layer can be 27°C. When the tunnel buried depth is larger than 11.4 m, the temperature of lining with thermal insulation layer in winter is mainly affected by the cold air in the tunnel. When the monthly and lowest daily mean air temperature are lower than −10°C and −14.3°C, respectively, in January, the temperature at the inner side of the 7 cm-thick thermal insulation layer is below 0°C.

(3) If the tunnel buried depth is less than 11.4 m, the temperature of lining is lower, resulting from the combined effect of low temperature in the tunnel and at ground surface. The thicker thermal insulation layer is needed. It is even necessary to take an appropriate active heating measure, if the buried depth is too shallow.

(4) The thermal insulation layer thickness needs to be calculated and designed considering the longitudinal air temperature distribution and the buried depth along the tunnel length, especially the long tunnel, in order to prevent tunnel lining frost and reduce engineering cost.

Data Availability

The field temperature test data used to support the findings of this study are included within the article.

Conflicts of Interest

The authors declare that there are no conflicts of interest regarding the publication of this paper.

Acknowledgments

The authors would like to acknowledge the financial support provided by the National Key R&D Program of China (Grant no. 2016YFC0802202); the National Natural Science Fund Project of China (Grant no. 51678063); the China Postdoctoral Science Foundation (Grant no. 2016M602738); and the Natural Science Basic Research Plan in Shaanxi Province of China (Grant no. 2017JM5051).

References

[1] C. Jianxun, Z. Xizhong, L. Yanbin, D. Xianghui, and L. Qin, “Investigating freeze-proof durability of C25 shotcrete,” *Construction & Building Materials*, vol. 61, pp. 33–40, 2014.

[2] J. X. Chen, X. H. Deng, Y. B. Luo, L. C. He, Q. Liu, and X. Qiao, “Investigation of microstructural damage in shotcrete under a freeze–thaw environment,” *Construction & Building Materials*, vol. 83, pp. 275–282, 2015.

[3] J. Chen, P. Zhao, Y. Luo, X. Deng, and Q. Liu, “Damage of shotcrete under freeze-thaw loading,” *Journal of Civil Engineering and Management*, vol. 23, no. 5, pp. 583–593, 2017.

[4] W. W. Liu, Q. Feng, C. X. Wang, C. K. Lu, Z. Z. Xu, and W. T. Li, “Analytical solution for three-dimensional radial heat transfer in a cold-region tunnel,” *Cold Regions Science and Technology*, vol. 164, pp. 1–12, 2019.

[5] G. M. Elliot, M. R. Sandfort, and J. C. May, “How to prevent tunnel ice-up,” *Tunnels &Tunnelling*, vol. 27, no. 11, pp. 42-43, 1995.

[6] A. Inokuma and S. Inano, “Road tunnels in Japan: deterioration and countermeasures,” *Tunnelling and Underground Space Technology*, vol. 11, no. 3, pp. 305–309, 1996.

[7] E. Broch, E. Grøv, and K. Inge Davik, “The inner lining system in Norwegian traffic tunnels,” *Tunnelling and Underground Space Technology*, vol. 17, no. 3, pp. 305–314, 2002.

[8] K.-J. Jun, Y.-C. Hwang, and C.-Y. Yune, “Field measurement of temperature inside tunnel in winter in Gangwon, Korea,” *Cold Regions Science and Technology*, vol. 143, pp. 32–42, 2017.

[9] Y.-M. Lai, Z. Wu, Y. Zhu, and L. Zhu, “Nonlinear analysis for the coupled problem of temperature and seepage fields in cold regions tunnels,” *Cold Regions Science and Technology*, vol. 29, no. 1, pp. 89–96, 1999.

[10] Y. Lai, Z. Wu, S. Zhang, W. Yu, and Y. Deng, “Study of methods to control frost action in cold regions tunnels,” *Journal of Cold Regions Engineering*, vol. 17, no. 4, pp. 144–152, 2003.

[11] J. Lai, J. Qiu, H. Fan, J. Chen, and Y. Xie, “Freeze-proof method and test verification of a cold region tunnel employing electric heat tracing,” *Tunnelling and Underground Space Technology*, vol. 60, pp. 56–65, 2016.

[12] G. Zhang, C. Xia, Y. Yang, M. Sun, and Y. Zou, “Experimental study on the thermal performance of tunnel lining ground heat exchangers,” *Energy and Buildings*, vol. 77, pp. 149–157, 2014.

[13] G. Zhang, C. Xia, X. Zhao, and S. Zhou, “Effect of ventilation on the thermal performance of tunnel lining GHEs,” *Applied Thermal Engineering*, vol. 93, pp. 416–424, 2016.

[14] Z. Xuefu, L. Yuanming, Y. Wenbing, and Z. Shujuan, “Nonlinear analysis for the three-dimensional temperature fields in cold region tunnels,” *Cold Regions Science and Technology*, vol. 35, no. 3, pp. 207–219, 2002.

[15] Z. Xuefu, L. Yuanming, Y. Wenbing, Z. Shujuan, and X. Jianzhang, “Forecast analysis of the refreezing of Kunlun mountain permafrost tunnel on Qing-Tibet railway in China,” *Cold Regions Science and Technology*, vol. 39, no. 1, pp. 19–31, 2004.

[16] Z. Xuefu, X. Jianzhang, Z. Yaonan, and X. Shengxie, “Study of the function of the insulation layer for treating water leakage in permafrost tunnels,” *Applied Thermal Engineering*, vol. 27, no. 2-3, pp. 637–645, 2007.

[17] J. X. Chen, “Technique of preventing frost damage in highway tunnel,” *Journal of Chang’an University (Natural Science Edition)*, vol. 26, no. 4, pp. 68–70, 2006, in Chinese.

[18] P. Qi, J. Zhang, Z. R. Mei, and Y. X. Wu, "Study on the range of freeze-thaw of surrounding rock from a cold-region tunnel and the effects of Insulation Material," *Advanced Materials Research*, vol. 399–401, pp. 2222–2225, 2011.

[19] Y. Zhou, X. Zhang, and J. Deng, "A mathematical optimization model of insulation layer's parameters in seasonally frozen tunnel engineering," *Cold Regions Science and Technology*, vol. 101, pp. 73–80, 2014.

[20] Q. Ma, X. Luo, Y. Lai, F. Niu, and J. Gao, "Numerical investigation on thermal insulation layer of a tunnel in seasonally frozen regions," *Applied Thermal Engineering*, vol. 138, pp. 280–291, 2018.

[21] H. Q. Xie, C. He, and Y. L. Li, "Study on insulating layer thickness by phase-change temperature field of highway tunnel in cold region," *Chinese Journal of Rock Mechanics and Engineering*, vol. 26, no. 2, pp. 4395–4401, 2007, in Chinese.

[22] X. Tan, W. Chen, G. Wu, and J. Yang, "Numerical simulations of heat transfer with ice-water phase change occurring in porous media and application to a cold-region tunnel," *Tunnelling and Underground Space Technology*, vol. 38, pp. 170–179, 2013.

[23] H. Song, C. L. Ye, and J. F. Mi, "Numerical analysis of optimization design for insulation layer in cold regions tunnel," *Advanced Materials Research*, vol. 1065–1069, pp. 368–372, 2015.

[24] S. Li, F. Niu, Y. Lai, W. Pei, and W. Yu, "Optimal design of thermal insulation layer of a tunnel in permafrost regions based on coupled heat-water simulation," *Applied Thermal Engineering*, vol. 110, pp. 1264–1273, 2017.

[25] Q. Y. Yan, B. J. Li, Y. Y. Zhang, J. Yan, and C. Zhang, "Numerical investigation of heat-insulating layers in a cold region tunnel, taking into account airflow and heat transfer," *Applied Science*, vol. 7, no. 7, p. 679, 2017.

[26] Q. Y. Yu, C. Zhang, Z. X. Dai, C. Du, M. R. Soltanian, and M. Soltanian, "Impact of tunnel temperature variations on surrounding rocks in cold regions," *Periodica Polytechnica Civil Engineering*, vol. 63, no. 1, pp. 160–167, 2019.

[27] Y. B. Luo, *Study on frost damage grades and its prevention and control technologies in cold region tunnel*, Ph.D. thesis, Beijing Jiaotong University, Beijing, China, 2010.

[28] Q. Feng and B. S. Jiang, "Analytical method for insulation layer thickness of highway tunnels with multilayer dielectric in cold regions," *Chinese Journal of Geotechnical Engineering*, vol. 36, no. 10, pp. 1779–1887, 2014, in Chinese.

[29] Q. Feng, B.-S. Jiang, Q. Zhang, and G. Wang, "Reliability research on the 5-cm-thick insulation layer used in the Yuximolegai tunnel based on a physical model test," *Cold Regions Science and Technology*, vol. 124, pp. 54–66, 2016.

[30] J. Lai, X. Wang, J. Qiu et al., "A state-of-the-art review of sustainable energy based freeze proof technology for cold-region tunnels in China," *Renewable and Sustainable Energy Reviews*, vol. 82, pp. 3554–3569, 2018.

[31] Y. B. Luo, J. .X. Chen, and M. .S. Wang, "Classification of frost damage grades in tunnel," *Journal of Beijing University of Technology*, vol. 36, no. 4, pp. 458–462, 2010, in Chinese.

[32] P. Y. Zhao, J. X. Chen, Y. B. Luo, X. B. Bu, L. J. Chen, and Y. Li, "Long-term, real-time and multi-channel distributed temperature monitoring system for tunnels in cold regions," *Measurement Science and Technology*, vol. 30, no. 6, pp. 1–11, 2019.

[33] Y. X. Shi, *Study on calculation method of natural wind and energy saving ventilation technology on tunnel*, Ph.D. thesis, Southwest Jiaotong University, Chengdu, China, 2011.

[34] F. Chao, M. N. Wang, L. Yu, and C. Guo, "A study on the natural wind calculation method and energy conservation in extra-long highway tunnels," *Modern Tunnelling Technology*, vol. 53, no. 1, pp. 111–118, 2016, in Chinese.

[35] Y. Kurokawa, "Current situation and problems of prevention and control of icicle in tunnel," *Transport and Underground*, vol. 11, no. 12, pp. 13–21, 1980, in Japanese.

[36] X. Tan, W. Chen, D. Yang et al., "Study on the influence of airflow on the temperature of the surrounding rock in a cold region tunnel and its application to insulation layer design," *Applied Thermal Engineering*, vol. 67, no. 1-2, pp. 320–334, 2014.

[37] C. C. Xia, D. F. Fan, Q. Li, and J. He, "An approach for determining length of insulation layer in cold region tunnels," *Journal of Tongji University (Natural Science)*, vol. 44, no. 9, pp. 1363–1370, 2016, in Chinese.

[38] JTG/T D31-06-2017, *Technical Specifications for Design and Construction of Highway in Seasonal Frozen Soil Region*, Ministry of Transport of the People's Republic of China, Beijing, China, 2017.

[39] Y. Gao, Y. Q. Zhu, D. P. Zhao, J. Y. Geng, and H. Xin, "Study on classified suggestion of tunnel in cold region and thermal insulation-considered drainage technology," *Chinese Journal of Rock Mechanics and Engineering*, vol. 37, no. 1, pp. 3489–3499, 2018, in Chinese.